Identification of bZIP Interaction Partners of Viral Proteins HBZ, MEQ, BZLF1, and K-bZIP Using Coiled-Coil Arrays[†]

Aaron W. Reinke, Gevorg Grigoryan, and Amy E. Keating*

Department of Biology, Massachusetts Institute of Technology, Cambridge, Massachusetts 02139

Received December 2, 2009; Revised Manuscript Received January 22, 2010

ABSTRACT: Basic-region leucine-zipper transcription factors (bZIPs) contain a segment rich in basic amino acids that can bind DNA, followed by a leucine zipper that can interact with other leucine zippers to form coiled-coil homo- or heterodimers. Several viruses encode proteins containing bZIP domains, including four that encode bZIPs lacking significant homology to any human protein. We investigated the interaction specificity of these four viral bZIPs by using coiled-coil arrays to assess self-associations as well as heterointeractions with 33 representative human bZIPs. The arrays recapitulated reported viral−human interactions and also uncovered new associations. MEQ and HBZ interacted with multiple human partners and had unique interaction profiles compared to any human bZIPs, whereas K-bZIP and BZLF1 displayed homospecificity. New interactions detected included HBZ with MAFB, MAFG, ATF2, CEBPG, and CREBZF and MEQ with NFIL3. These were confirmed in solution using circular dichroism. HBZ can heteroassociate with MAFB and MAFG in the presence of MARE-site DNA, and this interaction is dependent on the basic region of HBZ. NFIL3 and MEQ have different yet overlapping DNA-binding specificities and can form a heterocomplex with DNA. Computational design considering both affinity for MEQ and specificity with respect to other undesired bZIP-type interactions was used to generate a MEQ dimerization inhibitor. This peptide, anti-MEQ, bound MEQ both stably and specifically, as assayed using coiled-coil arrays and circular dichroism in solution. Anti-MEQ also inhibited MEQ binding to DNA. These studies can guide further investigation of the function of viral and human bZIP complexes.

Many viruses hijack cellular machinery by using viral proteins to interact with host proteins. Viruses can incorporate host protein domains into their genomes for this purpose, as is the case for several viruses that use BCL-2 homologues to prevent apoptosis. Viral host-derived protein domains often make interactions similar to those of their homologues, although these can occur in a misregulated manner (*1*). Alternatively, host-derived protein domains can diverge from their cellular counterparts, such that they retain little sequence similarity. In such cases, virus−host protein interactions can be expected to differ markedly from corresponding host−host complexes (*2*).

The bZIP[1] transcription factors are a large class of proteins found in most eukaryotic organisms. Named for their DNA-binding and dimerization domain, bZIP proteins interact with DNA site-specifically via a region of conserved basic amino acids. Immediately C-terminal to the basic region is the leucine zipper, a coiled coil that mediates the formation of homodimeric or heterodimeric complexes. The dimerization specificity of the leucine zippers allows for combinatorial interactions that can influence DNA binding and thus transcriptional regulation (*3, 4*). Given the importance of protein partnering specificity for the function of the bZIPs, a high-throughput protein array assay was used to determine the global *in vitro* interaction profiles of most human bZIPs. The coiled-coil microarray assay used for this purpose was shown to identify most reported interactions, and the relative stabilities of interactions measured on the arrays were also shown to agree well with solution measurements (*5, 6*).

Proteins containing bZIP domains have been identified in several viruses. Three human bZIP proteins, JUN (cJun), FOS (cFos), and MAF (cMaf), occur in an altered form in oncogenic avian and murine retroviruses. These homologous viral bZIPs maintain the protein dimerization properties of the human proteins and are oncogenic because of altered regulation (*7−9*). Four viral bZIPs that have little homology to human bZIPs have also been identified, and although several interactions with host proteins have been reported, global investigation of the interactions of these proteins with host bZIPs is lacking.

Human T-cell leukemia virus type 1 is a retrovirus that causes adult T-cell leukemia; it encodes the bZIP protein HBZ (reviewed in ref *10*). HBZ has been shown to repress both viral and cellular gene expression. A recent study suggests that, in addition to the role of the HBZ protein in disease progression, the mRNA of HBZ promotes proliferation (*11*). Interactions have been reported between HBZ and many human bZIPs both *in vivo* and *in vitro* including ATF4, JUN, JUNB, JUND, CREB1, ATF1,

and CREM (*12−15*). HBZ has been shown to form complexes with JUN, JUNB, CREB1, and ATF4 and to prevent these proteins from binding DNA. In contrast, HBZ has been reported to increase the transcriptional activity of JUND (*13*).

MEQ is encoded by Marek's disease virus (MDV), an oncogenic herpes virus that infects chickens. The disease is estimated to cost the U.S. poultry industry one billion dollars annually (reviewed in ref *16*). MEQ has been demonstrated to be largely responsible for the oncogenic properties of MDV (*17−19*). MEQ can self-associate as well as interact with a variety of other bZIPs *in vitro* including JUN, JUNB, CREB1, ATF1, ATF2, ATF3, FOS, and BATF3 (*17, 20−22*). Additionally, MEQ has been shown to bind JUN *in vivo*, and JUN is required for MEQ to transform cells (*18, 20*).

Two gamma herpes viruses are reported to encode bZIP-containing proteins. These viruses are implicated in several proliferative disorders in humans. Epstein−Barr virus encodes BZLF1 (ZEBRA, Zta, Z, EB1) and is associated with Burkitt's lymphoma, Hodgkin's disease, and nasopharyngeal carcinoma. Kaposi's sarcoma-associated herpes virus encodes K-bZIP (K8, RAP) and is involved in Kaposi's sarcoma, primary effusion lymphoma, and multicentric Castleman's disease (reviewed in refs *23* and *24*). These two proteins are positional homologues and also share low sequence similarity with one another (*25*). BZLF1 is responsible for triggering the switch from latent to lytic infection by binding sites within the viral genome and causing transcriptional activation of many genes. It is also involved in viral replication (*26, 27*). Overexpression of K-bZIP does not cause virus reactivation, but K-bZIP is necessary for viral replication as well as the repression and activation of many genes within the viral genome, though not always through direct binding to promoters (*28, 29*). BZLF1 and K-bZIP both interact with many viral and cellular proteins including the human bZIP CEBPA (C/EBPα) (*30*). Interestingly, the interaction with CEBPA for both BZLF1 and K-bZIP is proposed to involve higher order oligomers rather than just dimers (*31, 32*). Recently, the crystal structure of BZLF1 was solved showing that a C-terminal region adjacent to the leucine zipper folds back and stabilizes the coiled-coil structure, significantly stabilizing the homodimer (*33*). K-bZIP has been shown to self-associate through its leucine zipper, but this homomeric interaction was reported to be one of higher order oligomers (*25, 32*).

Given the importance of both human and viral bZIPs to human health, several strategies have been used to generate inhibitors that can prevent dimerization and/or DNA binding. One approach is to use the leucine zipper of a homodimerizing bZIP as a dominant negative. The utility of this approach has been demonstrated in the context of BZLF1. Using a peptide that consisted of only the leucine zipper of BZLF1 (*34*), Hicks et al. showed that BZLF1 could be prevented from binding DNA. However, the EC_{50} for the peptide was high micromolar. A possible disadvantage of using native leucine-zipper peptides as inhibitors is that these may associate with bZIPs other than the desired target. Recently, we reported a computational design method for obtaining peptides that interact specifically with leucine zippers and applied it to a range of human targets. Out of the 20 human bZIP families, peptides were designed that successfully interacted with 19. Of these 19, 8 designs bound to their target family stronger than to any other family (*5*).

Here we report all pairwise interactions of four bZIP peptides derived from viral proteins with 33 human bZIP proteins measured using peptide microarrays. We identified several new interactions for both MEQ and HBZ, and these interactions were confirmed using circular dichroism and gel-shift assays. Additionally, we designed a peptide, anti-MEQ, to serve as a MEQ dimerization inhibitor. We demonstrate that this peptide binds specifically to MEQ and can prevent MEQ from binding DNA.

EXPERIMENTAL PROCEDURES

Plasmid Construction, Protein Expression, and Purification. Human protein constructs used for array experiments have been previously described and are listed in Supporting Information Table S1 (*5, 6*). Synthetic genes encoding the leucine-zipper regions of HBZ, MEQ, BZLF1, K-bZIP, anti-MEQ and the full bZIP domains of MAFB, HBZ, and MEQ were synthesized using DNAWorks to design primers and a two-step PCR method to anneal them (*35*). The bZIP domains of CREBZF and ATF2 were cloned from plasmids acquired from Open Biosystems (*36*) and NFIL3, JUN, CEBPG, and MAFG were cloned from plasmids obtained from PlasmID (*37*). These proteins were cloned into modified versions of a pDEST17 vector. Proteins were expressed in *E. coli* RP3098 cells and purified under denaturing conditions using Ni-NTA followed by reverse-phase HPLC as described previously (*5, 6*). A tagless version of anti-MEQ used for gel-shift and CD studies was constructed by cloning into pSV282 (Vanderbilt University Medical Center, Center for Structural Biology). The 6×His-MBP-anti-MEQ fusion protein was expressed in RP3098 cells by growing a 1 L culture in LB at 37 °C and inducing at 0.5 OD by adding 1 mM IPTG and growing for 4 h. The fusion protein was purified under native conditions by binding to Ni-NTA resin (Qiagen) and eluted by adding 8 mL of buffer (300 mM imidazole, 20 mM Tris, 500 mM NaCl, 1 mM DTT, pH 7.9). The fusion protein was then dialyzed overnight into TEV cleavage buffer (50 mM Tris, 50 mM NaCl, 1 mM DTT, 0.5 mM EDTA, pH 7.5) and then cleaved by adding 100 μL of TEV protease (1 mg/mL) for 3 h at 18−22 °C. This mixture was then added to Ni-NTA resin and the flow-through collected. The anti-MEQ peptide was further purified using reverse-phase HPLC. The molecular weights of the peptides were confirmed by mass spectrometry. Protein sequences generated for this study are listed in Supporting Information Table S1.

Coiled-Coil Arrays. Array experiments were performed as described previously (*5*). The average background-corrected fluorescence values for all measurements are listed in Supporting Information Table S2. Two measures used to report fluorescence intensities in the figures are S_{array} and *arrayscore*. These are defined in refs *5* and *38*, respectively. S_{array} was calculated using the equation

$$S_{array}(a) = \frac{(a - \tilde{a})}{\sqrt{\sum_{i=1, a_i < \tilde{a}}^{N} (a_i - \tilde{a})^2 / N_{a < \tilde{a}}}}$$

where *a* was the average fluorescence intensity of a protein on the surface and $\tilde{a}$ was the median signal for all proteins on the surface interacting with the same solution probe, *N* was the number of proteins on the surface, and $N_{a < \tilde{a}}$ was the number of proteins with a value *a* below the median. The *arrayscore* values were calculated using the equation $-\log(F/F_{max})$, where *F* was the average fluorescence intensity of each protein on the surface

minus the median signal for all proteins on the surface interacting with the same solution protein, and F_{max} was the maximum F.

Circular Dichroism. Circular dichroism experiments were performed and T_ms fit as described previously (*5*). The concentrations used for each experiment are listed in the figure legends. Thermal dentaturations were measured from 0 to 65 °C, and all were reversible, with all complexes having differences in T_m of less than 3 °C upon refolding. The buffer for CD measurements of MEQ was PBS (12.5 mM potassium phosphate (pH 7.4) and 150 mM KCl) with 1 mM DTT. For measurements of HBZ the buffer also included 200 mM GdnHCl and 0.25 mM EDTA.

Phylogenetic Analysis. An unrooted phylogenetic tree was constructed using the neighbor-joining method for the 53 human and 4 viral bZIP leucine-zipper regions as described previously (*5*). For comparison of chicken and human sequences, each human bZIP was used to BLAST the *G. gallus* genome, and 41 chicken bZIPs were identified. Leucine-zipper regions were defined as previously reported (*6*). Families were defined according to evolutionary conservation and interaction profiles (*6*, *39*).

Gel-Shift Assay. DNA probes for the AP-1, TFIID, and NF-κB sites were obtained from Promega. Other probes were based on literature-defined sequences (MARE (*40*), CAAT (*41*), CRE1 (*20*), CRE2 (*42*), MDVORI (*20*)), ordered as PAGE-purified oligonucleotides (IDT), and then annealed. Probes were end labeled with $[\gamma\text{-}^{32}P]ATP$ using PNK (NEB). Proteins were incubated for 3 h at 18−22 °C in gel-shift buffer (50 mM KCl, 25 mM Tris, pH 8.0, 0.5 mM EDTA, 2.5 mM DTT, 1 mg/mL BSA, 10% (v/v) glycerol, 0.1 mg/mL competitor DNA (poly(I)·poly(C) (GE)). Radiolabeled DNA was then added and incubated for 1 h at 18−22 °C. Radiolabeled DNA was at a final concentration of 0.7 nM, except for experiments in Supporting Information Figure S4, where the final concentration was 20 nM. Protein/DNA mixtures were loaded on NOVEX DNA retardation gels (Invitrogen) using 0.5 × TBE buffer and run at 200−300 V for 15−25 min. For experiments involving the JUN protein, the buffer was precooled to 4 °C to prevent complex dissociation. Gels were dried and imaged using a phosphorimaging screen and a Typhoon 9400 imaging system.

Computational Design of Anti-MEQ. Anti-MEQ was designed using CLASSY with the HP/S/Ca energy function as previously reported (*5*). A total of 46 human proteins and design homodimerization were used as negative design states.

RESULTS

Four Unique bZIPs Are Encoded by Viral Genomes. There are four bZIPs of viral origin described in the literature that are not closely related to any human bZIP. These are MEQ, HBZ, BZLF1, and K-bZIP. To compare these proteins to the human bZIPs, a phylogenetic tree was constructed using the leucine-zipper regions of the four viral proteins as well as 53 human bZIPs (Figure 1A). According to this analysis, all four viral bZIPs are quite diverged from human bZIPs. The sequences of the four viral bZIPs are aligned to several representative human sequences in Figure 1B. Human bZIPs have a highly conserved basic region consisting of the motif (R/K)XX(R/K)N-(R/K)XAAXX(S/C)RX(R/K)(R/K) (*43*), and a striking feature of the basic-region alignment is the presence of an invariant asparagine in almost all human bZIPs. The only two human families that do not have this asparagine are CREBZF (ZF, Zhangfei) and DDIT3 (CHOP), which are not known to bind DNA as homodimers but can bind as heterodimers (*44*, *45*). An

arginine, separated by seven residues from the conserved asparagine, is strictly conserved in all human bZIPs. Both MEQ and BZLF1 conform well to this conserved motif and include the key asparagine and arginine residues. In contrast, the basic regions from HBZ and K-bZIP poorly match the basic-region motif, and neither contains the key conserved asparagine or arginine. The leucine-zipper regions of human bZIPs are four to seven heptads long and are characterized by strong conservation of leucine every seven amino acids. MEQ, HBZ, and to a lesser extent K-bZIP have mostly canonical leucine-zipper regions. On the other hand, BZLF1 has a very short leucine zipper that is noncanonical, with only one coiled-coil **d**-position leucine (coiled-coil residues are traditionally labeled **a**−**f**, with **a** and **d** largely buried in the core, **e** and **g** on the periphery, and **b**, **c**, and **f** on the outside of the helical complex). BZLF1 has also been shown to be stabilized by an extended C-terminal region that makes contacts with the coiled coil (*33*). These observations are consistent with reports of both MEQ and BZLF1 binding DNA, whereas there is no direct evidence to support binding of DNA by HBZ (*20*, *33*, *46*). K-bZIP has been shown to directly bind DNA, though it is not clear whether the bZIP domain is involved (*47*).

Unlike HBZ, K-bZIP, and BZLF1, which are found in viruses that infect humans, MEQ is encoded by an avian oncovirus. Because of the availability of a large number of human, but not avian, bZIP clones, we wanted to confirm that human bZIPs could be used as a reasonable substitute for chicken bZIPs. MEQ has been previously reported to interact with both human and mouse bZIP proteins (*20*). We also compared human bZIP sequences to chicken bZIP sequences and found them to be highly homologous (Supporting Information Figure S1). Considering just the coiled-coil interface positions that are most responsible for interactions (**adeg**), 85% of direct orthologues have greater than 90% identity. Additionally, all human bZIP families are conserved between human and chicken, except DDIT3, which is specific to humans.

Detection of Viral−Human bZIP Interactions. Interactions between human and viral bZIPs were measured using a previously described protein microarray assay (*5*, *6*). The leucine-zipper regions of 33 representative human bZIPs were purified and printed onto aldehyde-derivatized glass slides along with leucine zippers from the four viral proteins (Supporting Information Table S1). All human bZIP families were represented on the arrays except for OASISb, which is very similar in its protein sequences and interaction profiles to OASIS. Each protein was then individually fluorescently labeled and used to probe the arrays at a concentration of ∼160 nM, unless otherwise indicated. A total of eight spots on the surface were used for each measurement. The fluorescence intensity of each spot was corrected for background, and the averages of the eight values were converted into a score called S_{array}, a Z-score-like measure, as described previously (see Experimental Procedures and Supporting Information Table S2) (*5*).

As in prior studies using this technique, there were several indications that the data are of good quality. First, interactions observed among human bZIPs (measured simultaneously with the viral−human interaction data) were highly consistent with previously published data (Supporting Information Figure S2) (*6*). Next, each heteromeric interaction was measured twice, once when the first protein was on the surface and again when it was in solution. Most interactions were observed in both directions. Further, interactions involving MEQ and HBZ were measured over a large range of concentrations and gave rise to similar

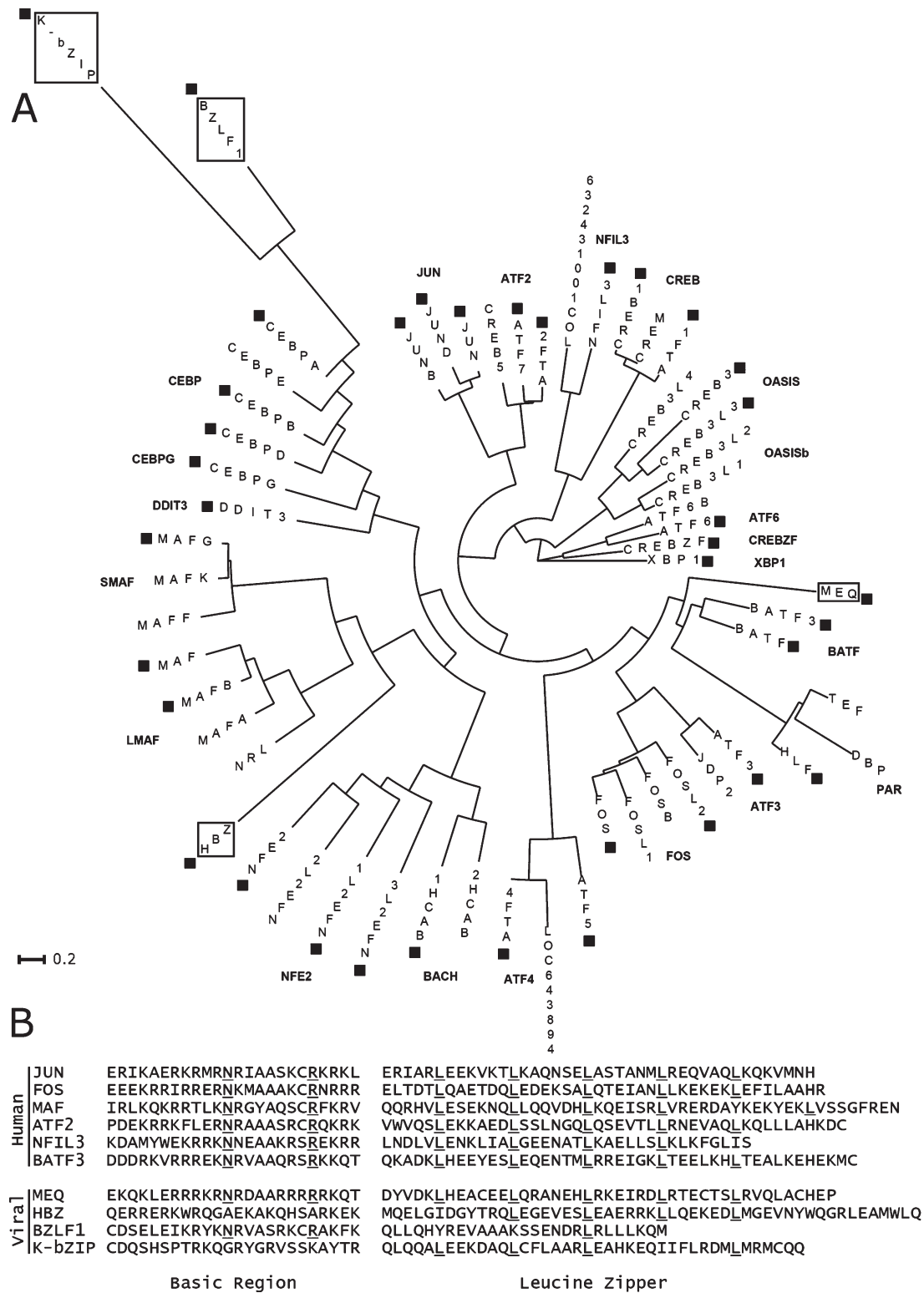|		Basic Region	Leucine Zipper
Human	JUN	ERIKAERKRMRNRIAASKCRKRKL	ERIARLEEKVKTLKAQNSELASTANMLREQVAQLKQKVMNH
	FOS	EEEKRRIRRERNKMAAAKCRNRRR	ELTDTLQAETDQLEDEKSALQTEIANLLKEKEKLEFILAAHR
	MAF	IRLKQKRRTLKNRGYAQSCRFKRV	QQRHVLESEKNQLLQQVDHLKQEISRLVRERDAYKEKYEKLVSSGFREN
	ATF2	PDEKRRKFLERNRAAASRCRQKRK	VWVQSLEKKAEDLSSLNGQLQSEVTLLRNEVAQLKQLLLAHKDC
	NFIL3	KDAMYWEKRRKNNEAAKRSREKRR	LNDLVLENKLIALGEENATLKAELLSLKLKFGLIS
	BATF3	DDDRKVRRREKNRVAAQRSRKKQT	QKADKLHEEYESLEQENTMLRREIGKLTEELKHLTEALKEHEKMC
Viral	MEQ	EKQKLERRRKRNRDAARRRRRKQT	DYVDKLHEACEELQRANEHLRKEIRDLRTECTSLRVQLACHEP
	HBZ	QERRERKWRQGAEKAKQHSARKEK	MQELGIDGYTRQLEGEVESLEAERRKLLQEKEDLMGEVNYWQGRLEAMWLQ
	BZLF1	CDSELEIKRYKNRVASRKCRAKFK	QLLQHYREVAAAKSSENDRLRLLLKQM
	K-bZIP	CDQSHSPTRKQGRYGRVSSKAYTR	QLQQALEEKDAQLCFLAARLEAHKEQIIFLRDMLMRMCQQ

FIGURE 1: Sequence properties of human and viral bZIPs. (A) A phylogenetic tree was inferred by neighbor joining using only the leucine-zipper region of each of the 53 human bZIPs and the 4 viral bZIPs. Viral sequences are boxed. Proteins used to measure interactions are indicated with a black square. Family names are in bold. The scale bar refers to amino acid changes per position. (B) Multiple-sequence alignment of viral bZIPs with representative human bZIPs. The following are underlined: highly conserved basic-region asparagine and arginine residues and conserved leucines in the leucine zippers.

interaction profiles (Figure 2B). Finally, many interactions observed between viral and human proteins were consistent with prior reports, as discussed below.

Most previously reported interactions involving the viral bZIPs were observed on the array and are indicated by green boxes in Figure 2A. Exceptions are boxed with green dotted lines

in Figure 2A and include the interaction of HBZ with ATF4 and the interaction of MEQ with FOS. However, the HBZ—ATF4 interaction was reported to be weaker with just the leucine-zipper region (as was measured on the arrays) than in context of the entire protein (*15*). Also, the interaction of MEQ with FOS has been shown to be weak compared to other interactions of
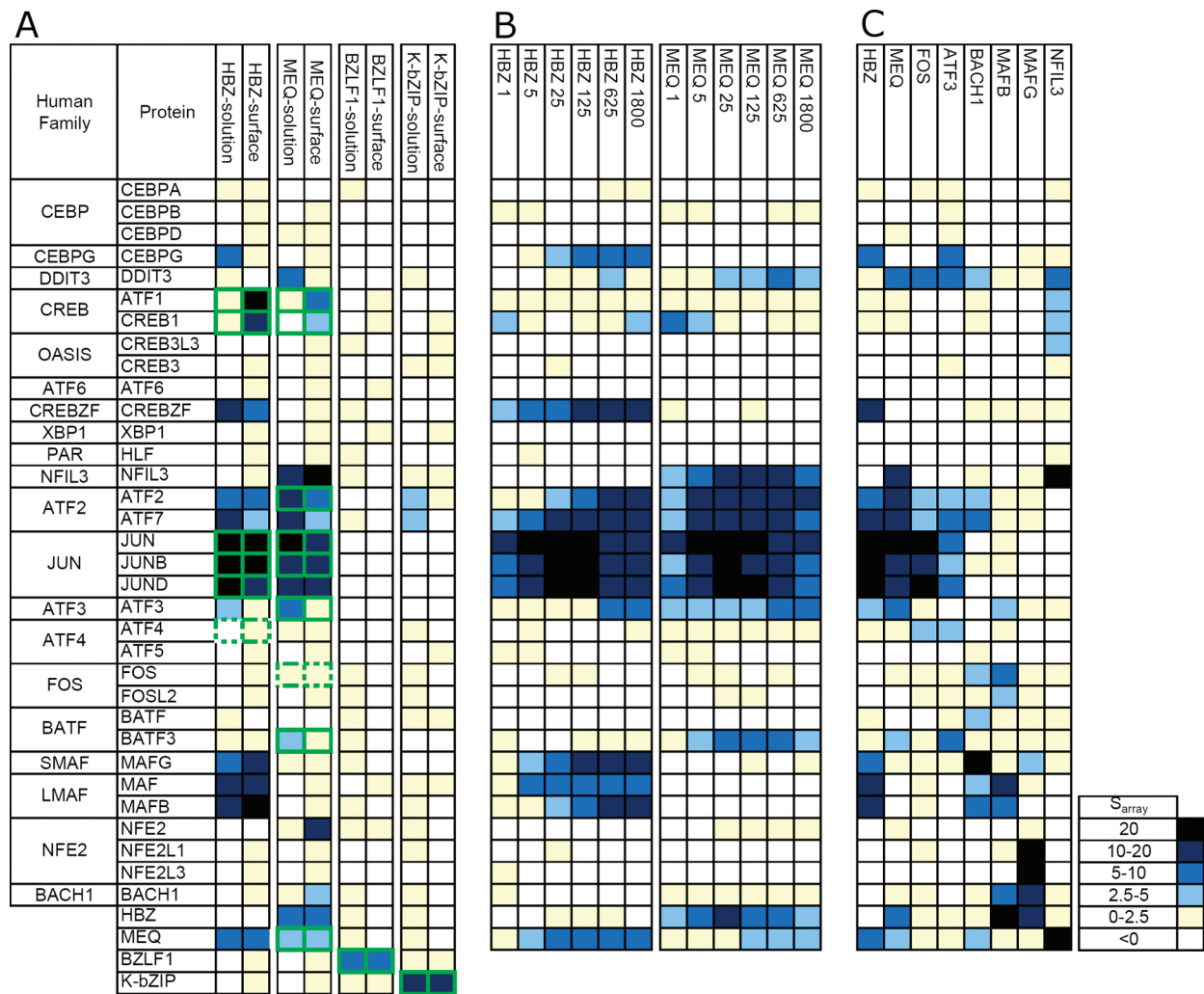
FIGURE 2: Identification of viral bZIP interactions using peptide microarrays. Interactions are displayed as a color map, as indicated by the scale at right. Family names are listed in the first column, and individual proteins are listed in the second column. (A) Interactions made by four viral proteins, when in solution or on the surface, are shown in columns. The potential interaction partners are in rows. Each heteromeric interaction is shown twice, corresponding to the two different ways it could be measured. Observations in agreement with prior studies are boxed in green; those interactions reported to be weak in the literature are indicated with dashed boxes. Fluorescently labeled proteins were used at 160 nM in a phosphate buffer that included 1 M guanidine hydrochloride (GdnHCl), except BZLF1 was used at a probe concentration of 1280 nM and K-bZIP was used at a probe concentration of 640 nM in 2.2 M GdnHCl. (B) MEQ and HBZ interactions at concentrations of 1−1800 nM. (C) Interaction profiles for six human proteins used as solution probes are shown for comparison to HBZ and MEQ solution profiles.

MEQ (*17*, *20*). Several interactions previously reported to not occur were also not observed on the arrays. These include HBZ self-interaction, HBZ—FOS, BZLF1—FOS, and BZLF1—JUN (*14*, *48*, *49*). Both BZLF1 and K-bZIP have been reported to interact with CEBPA, but not as heterodimers (see Discussion).

Many previously unreported interactions were detected for HBZ. New partners included MAF and MAFB, MAFG, ATF2 and ATF7, CEBPG (C/EBPγ), CREBZF, and ATF3. MEQ was observed to interact with JUND and ATF7, which are closely related to known partners JUN and ATF2, respectively. Other new interactions identified included MEQ with NFIL3 (E4BP4) and BACH1. Interactions were also observed for MEQ with DDIT3 and NFE2, but these proteins are not conserved between human and chicken. DDIT3 is a member of the one human bZIP family that is not found in chickens. The NFE2 family is conserved in chickens, but the human NFE2 protein does not have a direct orthologue, and the member of the family that does have a conserved orthologue, NFE2L1, is not observed to interact with MEQ.

BZLF1 was observed to self-associate strongly but not to interact with any human bZIP peptides (Figure 2A). A BZLF1 construct with the C-terminal extension (BZLF1CT) also did not interact strongly with any human proteins. This construct gave greater fluorescence signal when probed against itself than against the version containing just the leucine zipper. BZFL1CT also showed strong signal at a lower concentration than BZLF1 with just the leucine zipper. This result is consistent with previous reports documenting stabilities in solution and further demonstrates the ability of the arrays to accurately report relative affinities (Supporting Information Figure S3) (*34*, *50*). K-bZIP interacted with itself stronger than with any other protein on the arrays. Weak interactions were observed with ATF2 and ATF7 when K-bZIP was in solution, but these interactions were not observed when K-bZIP was on the surface (Figure 2A).

A significant result of this experiment is that the leucine-zipper regions of MEQ and HBZ participate in multiple interactions with different human bZIPs, while BZLF1 and K-bZIP display almost exclusive homoassociation (Figure 2A). Additionally, MEQ and HBZ each interact with a unique combination of

partners (Figure 2C). HBZ interacts with many of the same proteins as ATF3 and FOS but is distinguished by many other strong interactions that are not made by these proteins on the arrays, including interactions with both the small and large MAF families, CEBPG, and CREBZF. MEQ also has a similar profile to human ATF3 and FOS but additionally interacts strongly with NFIL3.

Validation of Novel Interactions of HBZ and MEQ in Solution. To validate novel interactions detected on the protein microarrays, we tested associations using circular dichroism (CD). Proteins consisting of the bZIP domain (basic region plus leucine zipper) were used for these experiments (see Experimental Procedures and Supporting Information Table S1). For NFIL3, the chicken and human proteins are identical in this region. For the MAF proteins, the extended homology region that contains an auxiliary DNA binding domain was included (*51*). We first tested JUN for interaction with HBZ and MEQ. JUN has been reported to interact with both MEQ and HBZ and was also observed to interact with both on the arrays. HBZ and JUN each at 40 μM were mixed together, and the CD spectrum was measured (Figure 3A). Spectra were also recorded for each protein in isolation. The spectra of each individual protein, as well as the mixture, had minima at 208 and 222 nm, which is characteristic of coiled coils. The observed mean residue elliptic-ity at 222 nm ($[\theta]_{222}$) is consistent with the expected helical content for these peptides forming coiled coils, as the leucine zipper accounts for ~50% of the sequence (*52*). The mixture also had increased signal compared to the sum of the individual proteins, indicating a heteroassociation. Similar results were observed for MEQ and JUN (Figure 3B).

We next tested HBZ against the newly identified partners ATF2, CEBPG, CREBZF, MAFG, and MAFB. Thermal melts monitored by CD were performed with each protein at a concentration of 4 μM and the mixture at 8 μM. Thermal melts were also carried out for HBZ with JUN (Figure 3C−H). Over a large range in temperature, all mixtures had increased signal over the sum of the spectra for the individual proteins, confirming the interactions. We then performed thermal melts of MEQ with NFIL3 and with JUN (Figure 3I,J). Again the mixture had increased signal over that expected for noninteracting proteins. Two pairs not observed to interact on the arrays, HBZ with NFIL3 and MEQ with MAFB, also were not observed to interact in solution (Figure 3K,L). Thus, all protein pairs tested in solution agreed well with the results of the protein array assay.

Characterization of HBZ Interactions with Human Proteins in the Presence of DNA. We tested whether HBZ could prevent its human bZIP interaction partners from binding DNA and/or whether heteromeric HBZ complexes could themselves bind DNA. MAFB and MAFG were tested in a gel-shift assay using a MARE site (*40*). Both bound MARE DNA as homo-dimers at a concentration of 4 nM, but HBZ did not bind even at a 100-fold higher concentration. Surprisingly, when highly purified HBZ at increasing concentrations was mixed with a constant concentration of either highly purified MAFB or MAFG, an additional shifted band of greater mobility appeared (Figure 4A). We inferred that this band included both HBZ and MAFB or MAFG. To determine whether formation of this complex was dependent on the basic region of HBZ, a leucine-zipper-only version of HBZ, HBZLZ, was mixed with the MAF proteins. The amount of MAF protein bound to DNA was decreased, though a higher concentration of HBZLZ was
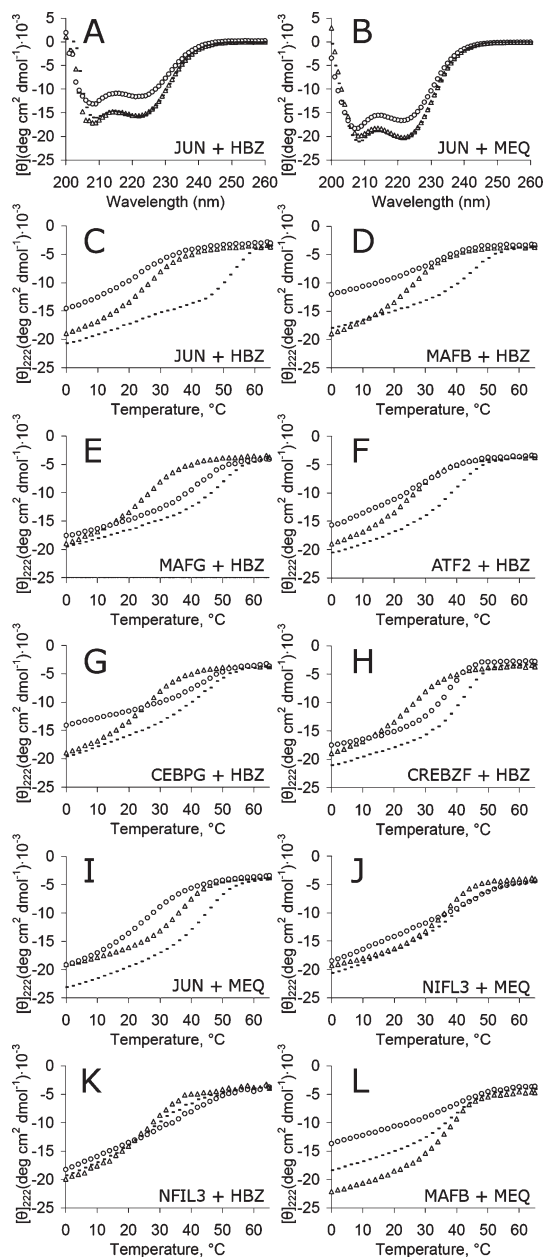
FIGURE 3: Solution measurements of novel interactions for HBZ and MEQ. (A, B) CD spectra at 40 μM for each protein or 80 μM for each mixture at 25 °C. (A) HBZ (open triangles), JUN (open circles), mixture (dashed line). (B) MEQ (open triangles), JUN (open circles), mixture (dashed line). (C−L) Thermal melts monitored by CD at 4 μM for each protein or 8 μM for each mixture. All mixtures are shown in dashed lines. (C) HBZ (open triangles), JUN (open circles). (D) HBZ (open triangles), MAFB (open circles). (E) HBZ (open triangles), MAFG (open circles). (F) HBZ (open triangles), ATF2 (open circles). (G) HBZ (open triangles), CEBPG (open circles). (H) HBZ (open triangles), CREBZF (open circles). (I) MEQ (open triangles), JUN (open circles). (J) MEQ (open triangles), NFIL3 (open circles). (K) HBZ (open triangles), NIFL3 (open circles). (L) MEQ (open triangles), MAFB (open circles).

required. No additional complex was detected (Figure 4B). This is the first evidence, to our knowledge, that HBZ can directly bind to DNA and that this binding depends on the basic region. The stoichiometry and structure of the observed heterocomplex remain unknown. We also tested whether ATF2 or CEBPG could bind DNA in complex with HBZ. Both ATF2 and CEBPG at 20 nM were prevented from binding MARE DNA by HBZ, but no additional band was formed (Figure 4C). CREBZF was
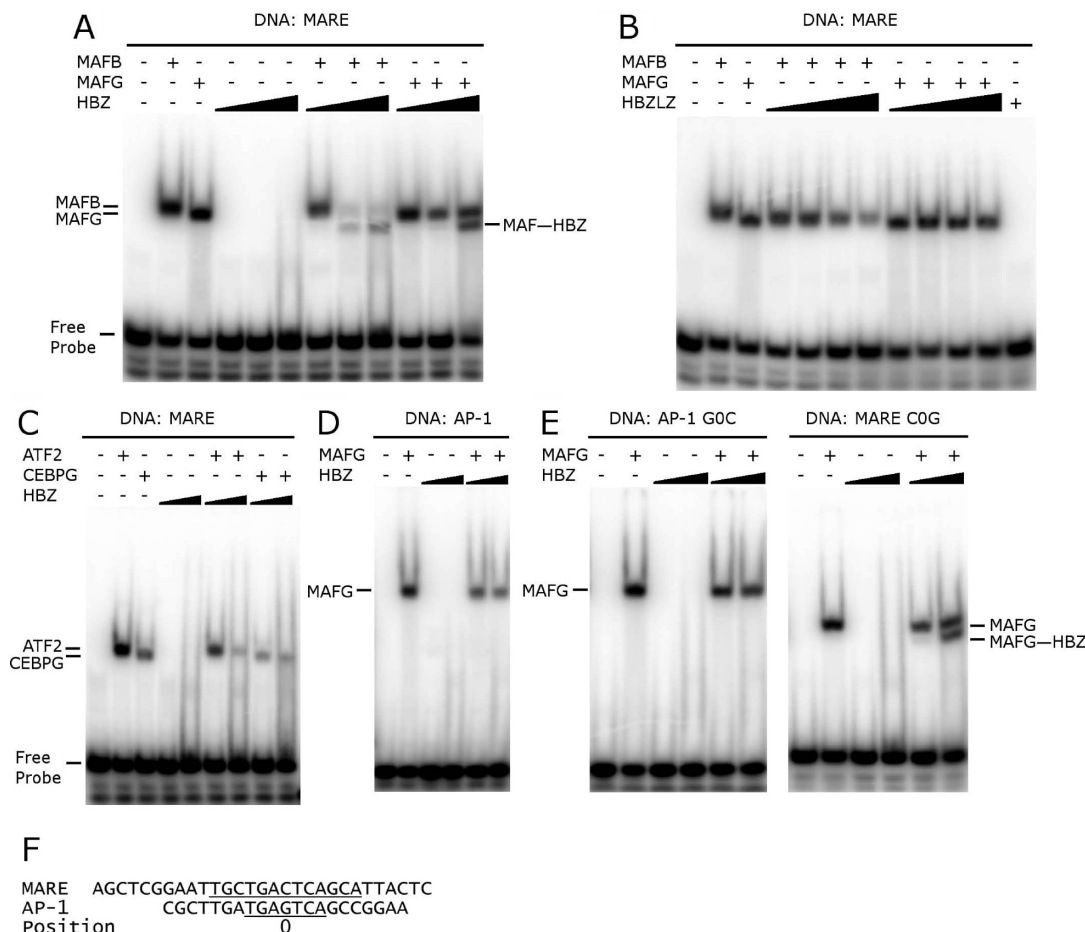
FIGURE 4: Binding of HBZ and human bZIPs to specific DNA sites assessed by gel shifts. Homo- and heterocomplexes formed on DNA are indicated. (A) HBZ can form heterocomplexes with MAFB or MAFG on MARE DNA sites. The concentration of MAFB was 4 nM, MAFG was 4 nM, and HBZ was 4, 40, or 400 nM. (B) A leucine-zipper-only version of HBZ (HBZLZ) prevents MAFB and MAFG from binding MARE-site DNA. The concentration of MAFB was 4 nM, MAFG was 4 nM, and HBZLZ was at 4, 40, 400, or 4000 nM. HBZLZ incubated alone was at 4000 nM. (C) HBZ prevents ATF2 and CEBPG from binding MARE-site DNA. The concentrations of ATF2 and CEBPG were 20 nM, and HBZ was at 40 or 400 nM. (D) HBZ prevents MAFG from binding AP-1 DNA. The concentration of MAFG was 20 nM, and HBZ was at 40 or 400 nM. (E) AP-1-site variant TGACTCA (G0C) was not sufficient for HBZ to bind DNA with MAFG. The concentration of MAFG was 20 nM with AP-1 G0C and 4 nM with MARE C0G. The concentration of HBZ was 40 or 400 nM. (F) DNA sequences used in gel-shift assays; the consensus site is underlined and position 0 is indicated.

not tested in complex with HBZ on DNA as CREBZF is not known to bind DNA by itself (*44*).

MAFG also binds to the AP-1 site. In contrast to the MARE site, HBZ decreased the binding of MAFG to the AP-1 site without formation of any additional shifted bands (Figure 4D). Both the AP-1 and the MARE sites contain the core consensus binding site TGA(C/G)TCA. The MAF proteins have an auxiliary binding domain that is responsible for binding flanking residues of the MARE site (*51*). At the middle of the binding site, position 0, the MARE site we used has a C and the AP-1 site contains a G. To determine if this middle position can affect DNA binding by HBZ—MAFG complexes, the 0 position in MARE was changed to a G and the same position in AP-1 was changed to a C. The mutant sites had similar binding properties to unchanged sites, suggesting that the middle position is not the key element that influences HBZ—MAFG heteroassociation on AP-1 vs MARE (Figure 4E,F). This suggests that bases flanking the core site are important for HBZ binding.

Characterization of MEQ and NFIL3 Binding to DNA. To determine whether NFIL3 and MEQ could bind DNA as heterodimers, we tested several known bZIP-binding sites. AP-1, also known as TRE, is a site bound by JUN and by FOS—JUN

heterodimer (*53*). CAAT contains the consensus site for the CEBP family of bZIPs (*54*). CRE1 and CRE2 are two CRE-like sites that have been previously used in DNA-binding studies with MEQ and NFIL3 and are each one change away from the consensus CRE site TGACGTCA (*20, 42*). Also tested was the MDVORI site, which is derived from the origin of replication of Marek's disease virus. MEQ has previously been shown to bind this site as a homodimer (*20*). In a gel-shift assay neither MEQ nor NFIL3 bound strongly to the negative control sites TFIID or NF-κB at 80 nM. Only MEQ bound strongly to the AP-1 site and only NFIL3 bound strongly to the CAAT site. Both MEQ and NFIL3 bound the CRE1 and CRE2 sites, though NFIL3 bound more strongly. For both of these sites there appeared to be some heterodimer formation, but the predominant species was the NFIL3 homodimer. Interestingly, NFIL3 bound to the MDVORI site, but weaker than MEQ did. The mixture of proteins bound to the MDVORI site was composed of primarily MEQ homodimers (Figure 5A).

We also wanted to know if MEQ and NFIL3 could bind a DNA site predominantly as a heterodimer. Previously it has been shown that heterodimer sites can be constructed by taking consensus half-sites for each of two interacting
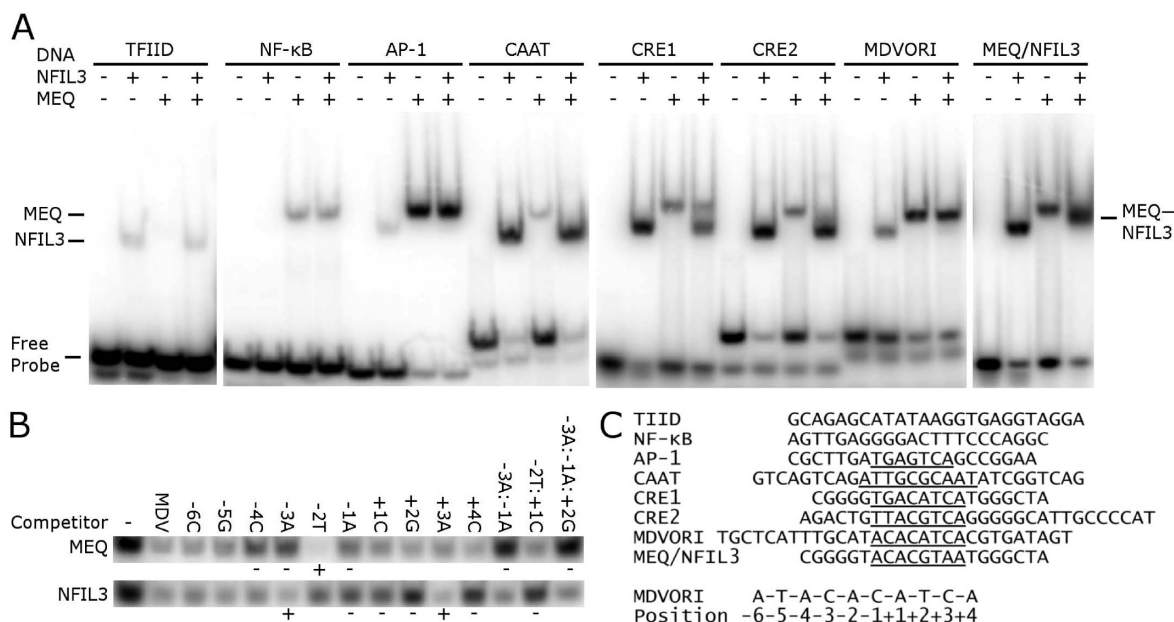
FIGURE 5: MEQ and NFIL3 interact and have different but overlapping DNA-binding specificities. (A) Gel-shift experiments with MEQ and NFIL3. The concentration of MEQ and NFIL3 was 80 nM each or 160 nM total protein for mixtures. Each homodimer and heterodimer is indicated. (B) Competition gel shift demonstrates that MEQ and NFIL3 bind to similar regions of an MDVORI probe but have differing specificities. Each protein was at 80 nM incubated with 0.7 nM radiolabeled MDVORI DNA. Above each lane is listed the mutation or mutations made in cold competitor DNA (400 nM). Three individual experiments were quantified, and those positions that gave ≥2-fold changes are indicated (± indicate increase/decrease in binding). (C) DNA sequences used in gel-shift assays; the consensus site is underlined. The positions of the MDVORI site are numbered.

bZIPs (*55*). A DNA site was constructed that contains the consensus half-sites for MEQ (ACAC) and NFIL3 (GTAA), referred to in Figure 5C and below as MEQ/NFIL3 (*20, 56*). This site has only two changes from the MDVORI site, at positions +1 and +3. This hybrid site was bound as a homodimer by both MEQ and NFIL3. NFIL3 bound tighter than MEQ, and when both proteins were mixed, the predominant species bound to the site was the hetero-complex, with mobility between the two homodimers (Figure 5A).

The MDVORI probe used in Figure 5 was 30 base pairs long, and to further probe the nature of a MEQ—NFIL3 interaction, we tested whether NFIL3 bound at a similar location as MEQ. Competition gel-shift experiments were performed to test this. MEQ and NFIL3 were individually incubated with radiolabeled MDVORI site and with cold competitor DNA encoding either the MDVORI site or a variant of it. Single-base substitutions were made at 10 consecutive positions in the site. Additionally, two double substitutions and a triple mutant site were constructed. Changes that affected MEQ binding by at least 2-fold were localized toward the 5′ half of the MDVORI site (Figure 5B). Substitutions that weakened MEQ binding included −4C, −3A, and −1A. The change of −2T strengthened MEQ binding. The double mutant of −3A:−1A decreased binding more than either individual substitution. NFIL3 binding was decreased by the changes −1A, +1C, +2G, and +4C. The substitutions −3A and +3A increased binding of NFIL3. Combining −2T and +1C decreased binding further. The changes of −1A and +2G decreased binding individually, but when both were together in combination with −3A, the triple mutant had no decrease in binding (Figure 5B). These 13 altered sites were also tested for direct binding to MEQ and NFIL3, and the results were consistent with the competition binding experiments (Supporting Information Figure S4). Additionally, significant

heterodimer formation by MEQ and NFIL3 was observed on the +3A site, consistent with results using the hybrid site in Figure 5A (Supporting Information Figure S4). Several things are apparent from this experiment. First, mutations on the 5′ side of the site affect binding to MEQ, while those toward the 3′ end, and at the last two positions of the left half-site, affect binding to NFIL3. Second, most DNA base changes have differential effects on the binding of MEQ and NFIL3, demonstrating they indeed have different binding specificities. Third, MEQ and NFIL3 bind at a similar location on the MDVORI DNA site.

Generation of a Specific Inhibitor of MEQ Dimerization. Specific inhibitors of bZIP interactions could provide valuable tools for elucidating function and could potentially serve to validate transcription factors as therapeutic targets. To generate a specific peptide to bind MEQ, that could potentially act as a dominant-negative inhibitor, we used a recently published computational design method called CLASSY (*5*). CLASSY was used to automatically design a peptide sequence predicted to bind MEQ but to have minimal binding to any human bZIP or to itself. The designed 42-residue anti-MEQ peptide was tested for its ability to bind MEQ using bZIP protein arrays including anti-MEQ, MEQ, and a panel of 32 human bZIPs (these included all the human peptides tested previously except DDIT3, which is specific to humans). Anti-MEQ bound MEQ stronger than any human protein (Figure 6A). The other proteins that anti-MEQ bound strongest are the ATF2 family proteins ATF2 and ATF7, followed by JUN and BATF3. Even at the highest concentration tested, 2000 nM, anti-MEQ bound MEQ and the ATF2 family proteins preferentially to other bZIPs. Anti-MEQ was not observed to interact with itself on the arrays. These results demonstrate that anti-MEQ is specific for binding to MEQ.

To compare the stability of the anti-MEQ—MEQ complex with that of other MEQ interactions, we probed MEQ against an
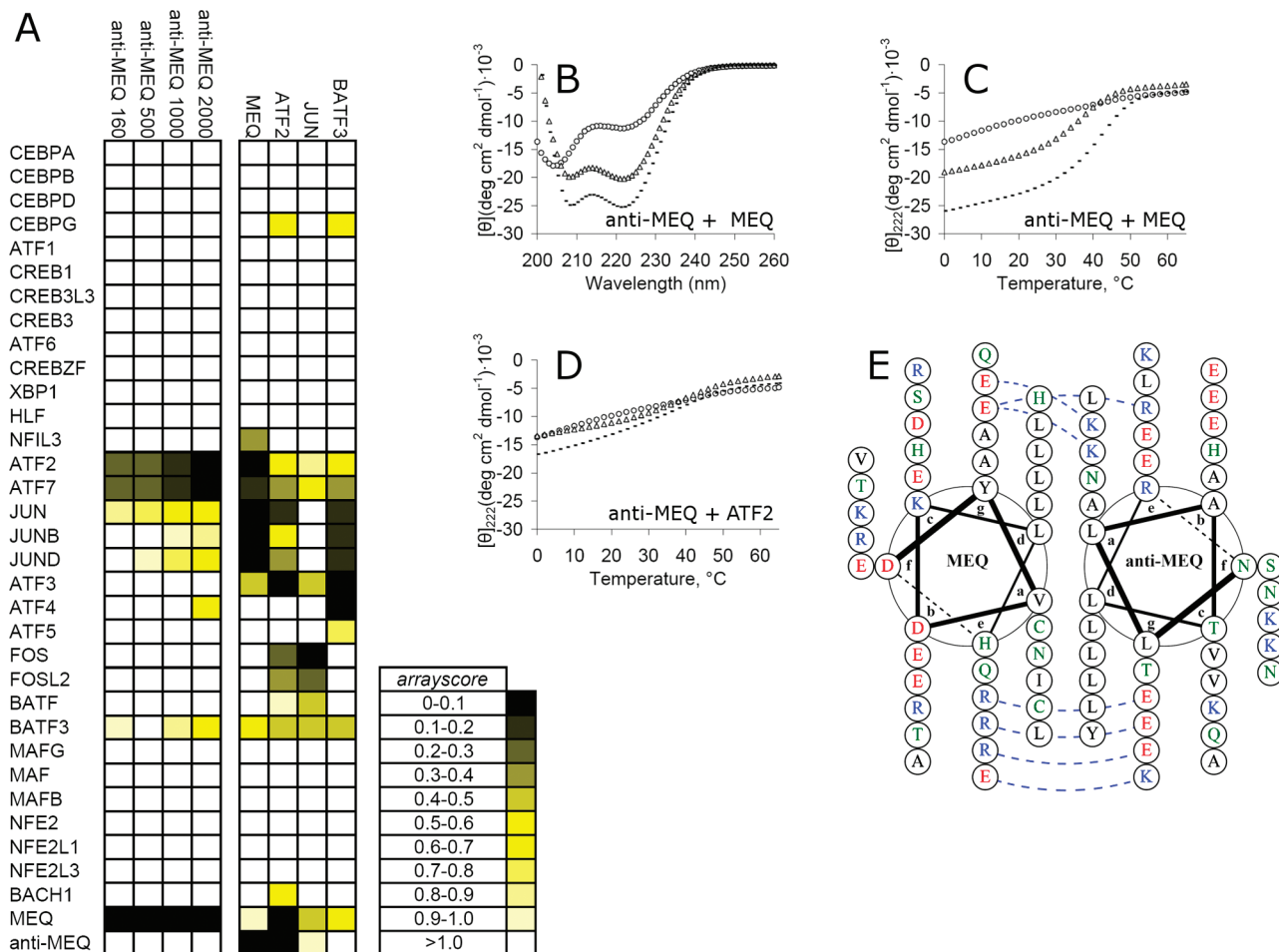
FIGURE 6: Anti-MEQ binds MEQ with high affinity and specificity. (A) Designed peptide anti-MEQ characterized using coiled-coil arrays. Color map of *arrayscore* is shown, with the colors defined in the scale. Left: anti-MEQ at different concentrations (nM) in solution is listed in columns, with proteins printed on the surface in rows. Right: MEQ and three human bZIPs tested against anti-MEQ and other proteins printed on the surface. (B) CD spectra at 40 μM for each protein or 80 μM for the mixture taken at 25 °C. MEQ (open triangles), anti-MEQ (open circles), and the mixture (dashed line). (C, D) Thermal melts monitored by CD at 4 μM for each protein or 8 μM for the mixture. (C) MEQ (open triangles), anti-MEQ (open circles), and the mixture (dashed line). (D) ATF2 (open triangles), anti-MEQ (open circles), and the mixture (dashed line). (E) Helical wheel diagram predicted for the interaction of MEQ with anti-MEQ. The complex is depicted as a parallel dimer, and the two helices of the coiled coil are shown from the N-terminus, with the sequence read clockwise and outward on each helix. Coiled-coil heptad positions are labeled. Hydrophobic residues are in black, charged residues are in red/blue, and polar residues are in green. Potential attractive electrostatic interactions are shown in dashed blue lines. Diagram created using DrawCoil 1.0 (http://www.gevorggrigoryan.com/drawcoil/).

array including MEQ, anti-MEQ, and the panel of 32 human peptides. MEQ interacted with anti-MEQ as strongly as it interacted with JUN, which was MEQ's strongest human interaction partner observed on the array (Figure 6A). The three strongest off-target interactions, ATF2, JUN, and BATF3, were also tested as solution probes. ATF2 bound anti-MEQ strongly compared to its strongest interactions on the array. In contrast, JUN and BATF had much weaker interactions with anti-MEQ. Overall, these results suggest that anti-MEQ has high affinity for, and is specific for, interaction with MEQ.

The interaction of MEQ and anti-MEQ in solution was studied using a tag-less version of anti-MEQ (see Experimental Procedures). CD spectra showed that anti-MEQ is mostly unfolded at 40 μM, and when combined with 40 μM MEQ the mixture has more signal than either MEQ or anti-MEQ alone, indicating an interaction. The mixture also has a spectrum characteristic of a coiled coil (Figure 6B). Thermal melts of anti-MEQ mixed with either MEQ or ATF2 were performed at 4 μM of each protein and 8 μM total protein for the mixture (Figure 6C,D). The temperature of half-denaturation (T_{m}) for

anti-MEQ was 12.8 °C, for MEQ was 35.2 °C, and for ATF2 was 36.7 °C. The T_{m} for anti-MEQ in complex with MEQ was 40.5 °C, and thus the heteroassociation is more stable than either the homoassociation of MEQ or anti-MEQ. The T_{m} of ATF2 in complex with MEQ was 31.8 °C. JUN, a strong interaction partner for MEQ, has a T_{m} in complex with MEQ of 41.3 °C. These results are consistent with the array data. A helical wheel diagram depicting the predicted interaction geometry of MEQ and anti-MEQ is shown in Figure 6E. The design has leucine residues at five consecutive **d**-positions, imparting stability to the complex (*57*). It also introduces a complementary asparagine residue to interact with an asparagine at an **a**-position in MEQ; this interaction is known to favor parallel dimer formation (*58*). The **e**- and **g**-positions of anti-MEQ are complementary to those in MEQ, and two rather uncommon cysteine residues at **a**-positions are predicted to lie across from designed alanine and lysine residues. Lysine at core **a**-positions also favors dimer formation (*59*). Two lysines at **a**-positions are complementary to glutamate residues at the **g**-position on the opposite helix. These **a**–**g**′ interactions have previously been postulated to make important contributions to specificity (*5, 38*).
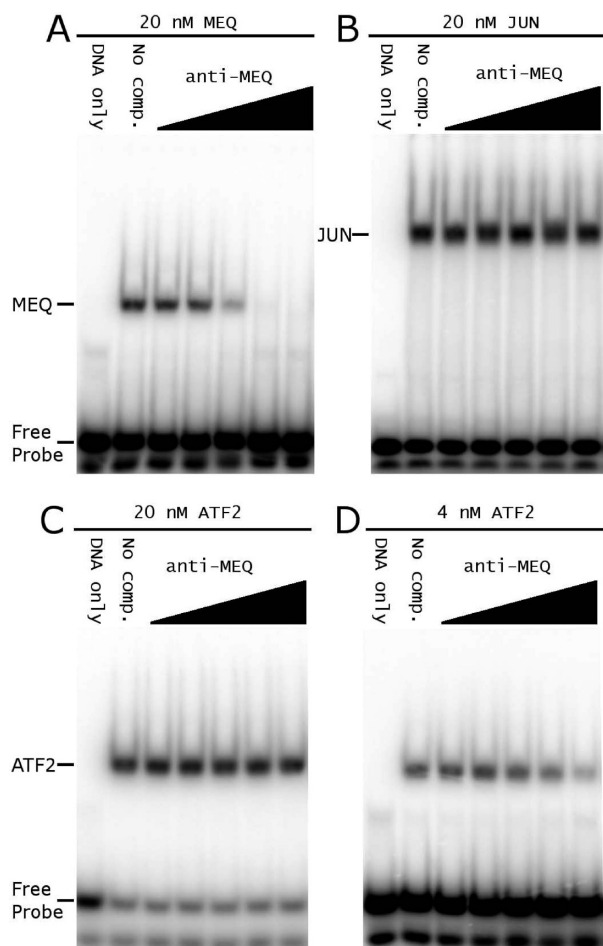
FIGURE 7: Anti-MEQ prevents MEQ from binding DNA. Competition gel shifts with a constant amount of the indicated protein bound to DNA were titrated with increasing amounts of anti-MEQ. Concentrations of competitor peptide were 0.02, 0.1, 0.5, 2.5, and 12.5 μM. Labeled DNA was present at 0.7 nM. (A) 20 nM MEQ with MDVORI DNA. (B) 20 nM JUN with AP-1 DNA. (C) 20 nM ATF2 with CRE2 DNA. (D) 4 nM ATF2 with CRE2 DNA.

To test whether anti-MEQ could prevent MEQ from binding DNA, 20 nM MEQ was incubated with increasing amounts of anti-MEQ, and then radiolabeled MDVORI DNA was added to the reactions. Anti-MEQ prevented MEQ binding of DNA, with an IC_{50} of less than 500 nM (Figure 7A). Binding of MEQ to AP-1 DNA was also inhibited by anti-MEQ (data not shown). The experiment was repeated with 20 nM JUN and the AP-1 DNA site. No decrease in JUN binding was observed even at 12.5 μM anti-MEQ (Figure 7B). The strongest off-target interaction for anti-MEQ, ATF2, was also tested. At 20 nM ATF2 no decrease in binding was observed when incubated with anti-MEQ (Figure 7C). At 4 nM ATF2, anti-MEQ decreased ATF2 binding, but at higher concentrations than required for preventing MEQ binding (Figure 7D). These results show that anti-MEQ can prevent MEQ from binding DNA at a lower concentration than it inhibits its strongest off-target interaction.

DISCUSSION

The bZIP transcription factors function by forming homodimers or heterodimers with other bZIP proteins. In this context, viruses use bZIP proteins in a number of distinct ways that are illuminated by the systematic study we present here. Several viral bZIPs that have high sequence identity to host homologues

maintain the interaction patterns of the host bZIPs. Examples include v-FOS, v-JUN, and v-MAF (7−9). The viral bZIPs HBZ and MEQ are not closely related to any other bZIPs, and they have distinct interaction profiles compared to the human bZIPs. K-bZIP and BZLF1 are also not highly conserved, but the bZIP domains of these two viral proteins primarily self-associate.

For MEQ and HBZ, we have uncovered new interactions that suggest possible mechanisms of action of these proteins. The mechanism of HBZ protein function has been somewhat of a mystery. The noncanonical basic region of this protein argues against direct DNA binding, yet HBZ was shown previously to have a strong activation domain, suggesting that it might function to regulate transcription when complexed with human bZIP proteins and DNA (15, 60). Additionally, HBZ has been shown to stimulate the transcriptional activity of JUND (13). However, data so far have not supported a direct interaction of HBZ itself with DNA. Here we present the first evidence that HBZ can directly bind DNA. HBZ can bind a MARE DNA site with MAFB or MAFG. This binding of DNA is specific and is dependent both on the HBZ basic region and on DNA that flanks the central binding site. While most bZIPs bind a four to five base pair half-site, different flanking regions around an AP-1 site have previously been shown to have different affinities for binding to JUN−FOS heterodimers (61). The HBZ ternary complex that we observed on DNA with either MAFB or MAFG was weaker than MAF−DNA complexes. Also, the HBZ−MAF complexes occurred at higher concentrations of HBZ relative to MAF protein. Because the sequence of the HBZ basic region is unique, it may have a distinct DNA-binding specificity, and it remains a possibility that higher affinity sites for HBZ in association with MAF proteins exist.

The MAF proteins belong to two classes: the four large MAF proteins, which contain a transcriptional activation domain, and the three small MAF proteins that do not. The small MAFs interact with the NFE2 and BACH families of bZIPs and play a major role in the response to oxidative stress (62). The large MAF proteins are similar to the JUN proteins in that both are involved in cell growth and proliferation, both are protooncogenes and can cause cellular transformation, and both have retroviral homologues (63, 64). They also have been reported to share similar downstream targets in inducing cellular transformation (65).

Other proteins we confirmed to interact with HBZ *in vitro* are CEBPG, ATF2, and CREBZF. The CEBP family of bZIPs is involved in cell growth and differentiation. CEBPG forms heterodimers with CEBP family proteins to repress their transcriptional activity (66). ATF2 has been shown to stimulate JUN-mediated cellular transformation (67). CREBZF was identified as having a role in herpes simplex virus gene expression (68). CREBZF also interacts with ATF4, a known partner of HBZ (15, 44). With ATF2 and CEBPG, it remains to be seen whether HBZ heterodimers can bind DNA sites or if HBZ functions primarily by preventing binding of these partners to target sites. Neither HBZ nor CREBZF has been shown to bind DNA as homodimers, suggesting that they have intrinsically weaker affinities for DNA and together would not be likely to bind DNA as a heterodimer. These newly reported partners, along with other known partners, suggest that HBZ has the potential to impact several different transcriptional pathways.

It was recently shown that MEQ homodimers alone are not sufficient to induce transformation, suggesting that heterodimer formation with other bZIPs is necessary (17). JUN has been

shown to be an important MEQ partner, required for cellular transformation mediated by MEQ, but it is likely that other interaction partners are also functionally important. Here we identified a previously unreported bZIP partner, NFIL3, and showed that it can form heterodimers with MEQ on DNA. NFIL3 was first identified as a transcriptional repressor that bound the adenovirus E4 promoter and was later shown to have an activating role associated with antiapoptotic activity. NFIL3 is also involved in regulating circadian rhythms (*56, 69, 70*). NFIL3 was further shown to repress both hepatitis B viral gene expression and replication (*71*). In this context, it is interesting that NFIL3 can bind to the MDVORI site as a homodimer. The MDVORI site from the origin of replication of MDV is also located near a bidirectional promoter that MEQ has been shown to repress as a homodimer (*20, 21*). There may exist functionally significant sites that MEQ and NFIL3 can bind as a heterodimer with greater affinity than either homodimer. It will be important to determine what role NFIL3 has on the MDV life cycle, both alone and in combination with MEQ.

Other novel interactions with bZIP families detected on the arrays but not tested further are HBZ with ATF3 and MEQ with BACH1. Based on the intensity of the fluorescence signal, these interactions are likely to be weaker than the other interactions tested, but they may be significant. Also, numerous interactions that we did not assay are highly likely to occur involving paralogues of the proteins tested here. Although these interactions need to be confirmed experimentally, most bZIP paralogues are highly similar to each other and have been shown to share similar interaction profiles (*5, 6, 39*).

An interesting result is that the leucine-zipper regions of BZLF1 and K-bZIP preferentially self-associate. Both proteins are reported to interact with CEBPA, but this pairing was not observed in our array experiments. Basic residues were required for this interaction in the case of BZLF1, and both proteins were observed to interact with CEBPA as higher order multimers and not as heterodimers (*31, 32*). Our observation that the leucine zippers are not sufficient for these interactions is consistent with those studies. It is not surprising, given the unique structure of BZLF1, that it does not form canonical interactions with human bZIPs.

MDV is the first oncogenic virus for which a vaccine was made available to control the disease, but increasing viral resistance is becoming a real concern to the poultry industry. Further, MDV has proven valuable as a model oncogenic virus, and deletion and knockdown experiments have demonstrated the necessity of MEQ for oncogenic transformation (*18*). It has also been reported that a virus encoding a MEQ protein that cannot form homodimers or heterodimers has a complete loss of oncogenicity, suggesting that the function of MEQ could be inhibited by preventing MEQ from interacting with bZIPs (*19*). We showed that a computationally designed anti-MEQ peptide can prevent MEQ from binding DNA in a specific manner, indicating that anti-MEQ could be a useful reagent for studying the role of MEQ on the oncogenic properties of MDV. If necessary to achieve higher affinity, the anti-MEQ peptide could potentially be further stabilized through the addition of an acidic peptide extension that interacts with the basic region, as has been demonstrated for numerous other coiled coils by the Vinson laboratory (*41*).

In summary, we have shown that coiled-coil arrays are a powerful method for broadly surveying the interaction properties of viral bZIP dimerization domains. Comprehensive testing for *in vitro* interactions with all human bZIP families is an important step in exploring the functions of these proteins. Further, we have validated that several newly discovered viral—host complexes can bind to DNA, suggesting a mechanism by which viruses hijack cellular transcriptional control. Determining which of the bZIPs that can associate *in vitro* also interact with functional consequences *in vivo* will be an important next step.

SUPPORTING INFORMATION AVAILABLE

Sequences of proteins used, comparison of human and chicken bZIP sequences, and additional coiled-coil array and gel-shift experiments. This material is available free of charge via the Internet at http://pubs.acs.org.

REFERENCES

1. Hardwick, J. M., and Bellows, D. S. (2003) Viral versus cellular BCL-2 proteins. *Cell. Death Differ. 10* (Suppl. 1), S68–S76.
2. Kvansakul, M., Yang, H., Fairlie, W. D., Czabotar, P. E., Fischer, S. F., Perugini, M. A., Huang, D. C., and Colman, P. M. (2008) Vaccinia virus anti-apoptotic F1L is a novel Bcl-2-like domain-swapped dimer that binds a highly selective subset of BH3-containing death ligands. *Cell. Death Differ. 15*, 1564–1571.
3. Daury, L., Busson, M., Tourkine, N., Casas, F., Cassar-Malek, I., Wrutniak-Cabello, C., Castellazzi, M., and Cabello, G. (2001) Opposing functions of ATF2 and Fos-like transcription factors in c-Jun-mediated myogenin expression and terminal differentiation of avian myoblasts. *Oncogene 20*, 7998–8008.
4. Hai, T., and Curran, T. (1991) Cross-family dimerization of transcription factors Fos/Jun and ATF/CREB alters DNA binding specificity. *Proc. Natl. Acad. Sci. U.S.A. 88*, 3720–3724.
5. Grigoryan, G., Reinke, A. W., and Keating, A. E. (2009) Design of protein-interaction specificity gives selective bZIP-binding peptides. *Nature 458*, 859–864.
6. Newman, J. R. S., and Keating, A. E. (2003) Comprehensive identification of human bZIP interactions with coiled-coil arrays. *Science 300*, 2097–2101.
7. van Straaten, F., Muller, R., Curran, T., Van Beveren, C., and Verma, I. M. (1983) Complete nucleotide sequence of a human c-onc gene: deduced amino acid sequence of the human c-fos protein. *Proc. Natl. Acad. Sci. U.S.A. 80*, 3183–3187.
8. Bos, T. J., Rauscher, F. J., III, Curran, T., and Vogt, P. K. (1989) The carboxy terminus of the viral Jun oncoprotein is required for complex formation with the cellular Fos protein. *Oncogene 4*, 123–126.
9. Kataoka, K., Nishizawa, M., and Kawai, S. (1993) Structure-function analysis of the maf oncogene product, a member of the b-Zip protein family. *J. Virol. 67*, 2133–2141.
10. Mesnard, J. M., Barbeau, B., and Devaux, C. (2006) HBZ, a new important player in the mystery of adult-T-cell leukemia. *Blood 108*, 3979–3982.
11. Satou, Y., Yasunaga, J.-i., Yoshida, M., and Matsuoka, M. (2006) HTLV-I basic leucine zipper factor gene mRNA supports proliferation of adult T cell leukemia cells. *Proc. Natl. Acad. Sci. U.S.A. 103*, 720–725.
12. Lemasson, I., Lewis, M. R., Polakowski, N., Hivin, P., Cavanagh, M.-H., Thebault, S., Barbeau, B., Nyborg, J. K., and Mesnard, J.-M. (2007) Human T-cell leukemia virus type 1 (HTLV-1) bZIP protein interacts with the cellular transcription factor CREB to inhibit HTLV-1 transcription. *J. Virol. 81*, 1543–1553.
13. Thebault, S., Basbous, J., Hivin, P., Devaux, C., and Mesnard, J.-M. (2004) HBZ interacts with JunD and stimulates its transcriptional activity. *FEBS Lett. 562*, 165–170.
14. Basbous, J., Arpin, C., Gaudray, G., Piechaczyk, M., Devaux, C., and Mesnard, J.-M. (2003) The HBZ factor of human T-cell leukemia virus type I dimerizes with transcription factors JunB and c-Jun and modulates their transcriptional activity. *J. Biol. Chem. 278*, 43620–43627.

15. Gaudray, G., Gachon, F., Basbous, J., Biard-Piechaczyk, M., Devaux, C., and Mesnard, J.-M. (2002) The complementary strand of the human T-cell leukemia virus type 1 RNA genome encodes a bZIP transcription factor that down-regulates viral transcription. *J. Virol. 76*, 12813–12822.

16. Nair, V. (2005) Evolution of Marek's disease—A paradigm for incessant race between the pathogen and the host. *Vet. J. 170*, 175–183.

17. Suchodolski, P. F., Izumiya, Y., Lupiani, B., Ajithdoss, D. K., Gilad, O., Lee, L. F., Kung, H.-J., and Reddy, S. M. (2009) Homodimerization of Marek's disease virus-encoded Meq protein is not sufficient for transformation of lymphocytes in chickens. *J. Virol. 83*, 859–869.

18. Levy, A. M., Gilad, O., Xia, L., Izumiya, Y., Choi, J., Tsalenko, A., Yakhini, Z., Witter, R., Lee, L., Cardona, C. J., and Kung, H.-J. (2005) Marek's disease virus Meq transforms chicken cells via the v-Jun transcriptional cascade: a converging transforming pathway for avian oncoviruses. *Proc. Natl. Acad. Sci. U.S.A. 102*, 14831–14836.

19. Brown, A. C., Smith, L. P., Kgosana, L., Baigent, S. J., Nair, V., and Allday, M. J. (2009) Homodimerization of the Meq viral oncoprotein is necessary for induction of T-cell lymphoma by Marek's disease virus. *J. Virol. 83*, 11142–11151.

20. Levy, A. M., Izumiya, Y., Brunovskis, P., Xia, L., Parcells, M. S., Reddy, S. M., Lee, L., Chen, H.-W., and Kung, H.-J. (2003) Characterization of the chromosomal binding sites and dimerization partners of the viral oncoprotein Meq in Marek's disease virus-transformed T cells. *J. Virol. 77*, 12841–12851.

21. Qian, Z., Brunovskis, P., Lee, L., Vogt, P. K., and Kung, H. J. (1996) Novel DNA binding specificities of a putative herpesvirus bZIP oncoprotein. *J. Virol. 70*, 7161–7170.

22. Qian, Z., Brunovskis, P., Rauscher, F., III, Lee, L., and Kung, H. J. (1995) Transactivation activity of Meq, a Marek's disease herpesvirus bZIP protein persistently expressed in latently infected transformed T cells. *J. Virol. 69*, 4037–4044.

23. Thomas, F. S. (2006) The pleiotropic effects of Kaposi's sarcoma herpesvirus. *J. Pathol. 208*, 187–198.

24. Kutok, J. L., and Wang, F. (2006) Spectrum of Epstein-Barr virus-associated diseases. *Annu. Rev. Pathol: Mech. Dis. 1*, 375–404.

25. Lin, S.-F., Robinson, D. R., Miller, G., and Kung, H.-J. (1999) Kaposi's sarcoma-associated herpesvirus encodes a bZIP protein with homology to BZLF1 of Epstein-Barr virus. *J. Virol. 73*, 1909–1917.

26. Countryman, J., Jenson, H., Seibl, R., Wolf, H., and Miller, G. (1987) Polymorphic proteins encoded within BZLF1 of defective and standard Epstein-Barr viruses disrupt latency. *J. Virol. 61*, 3672–3679.

27. Schepers, A., Pich, D., and Hammerschmidt, W. (1996) Activation of oriLyt, the lytic origin of DNA replication of Epstein-Barr virus, by BZLF1. *Virology 220*, 367–376.

28. Rossetto, C., Yamboliev, I., and Pari, G. S. (2009) Kaposi's sarcoma-associated herpesvirus/human herpesvirus 8 K-bZIP modulates LANA mediated suppression of lytic origin-dependent DNA synthesis, J. Virol., JVI.00922−00909.

29. Ellison, T. J., Izumiya, Y., Izumiya, C., Luciw, P. A., and Kung, H.-J. (2009) A comprehensive analysis of recruitment and transactivation potential of K-Rta and K-bZIP during reactivation of Kaposi's sarcoma-associated herpesvirus. *Virology 387*, 76–88.

30. Sinclair, A. J. (2003) bZIP proteins of human gammaherpesviruses. *J. Gen. Virol. 84*, 1941–1949.

31. Wu, F. Y., Wang, S. E., Chen, H., Wang, L., Hayward, S. D., and Hayward, G. S. (2004) CCAAT/enhancer binding protein {alpha} binds to the Epstein-Barr virus (EBV) ZTA protein through oligomeric interactions and contributes to cooperative transcriptional activation of the ZTA promoter through direct binding to the ZII and ZIIIB motifs during induction of the EBV lytic cycle. *J. Virol. 78*, 4847–4865.

32. Wu, F. Y., Wang, S. E., Tang, Q.-Q., Fujimuro, M., Chiou, C.-J., Zheng, Q., Chen, H., Hayward, S. D., Lane, M. D., and Hayward, G. S. (2003) Cell cycle arrest by Kaposi's sarcoma-associated herpesvirus replication-associated protein is mediated at both the transcriptional and posttranslational levels by binding to CCAAT/enhancer-binding protein {alpha} and p21CIP-1. *J. Virol. 77*, 8893–8914.

33. Petosa, C., Morand, P., Baudin, F., Moulin, M., Artero, J.-B., and Muller, C. W. (2006) Structural basis of lytic cycle activation by the Epstein-Barr virus ZEBRA protein. *Mol. Cell 21*, 565–572.

34. Hicks, M. R., Al-Mehairi, S. S., and Sinclair, A. J. (2003) The zipper region of Epstein-Barr virus bZIP transcription factor Zta is necessary but not sufficient to direct DNA binding. *J. Virol. 77*, 8173–8177.

35. Hoover, D. M., and Lubkowski, J. (2002) DNAWorks: an automated method for designing oligonucleotides for PCR-based gene synthesis. *Nucleic Acids Res. 30*, e43.

36. Gerhard, D. S., Wagner, L., Feingold, E. A., Shenmen, C. M., Grouse, L. H., Schuler, G., Klein, S. L., Old, S., Rasooly, R., Good, P., Guyer, M., Peck, A. M., Derge, J. G., Lipman, D., Collins, F. S., Jang, W., Sherry, S., Feolo, M., Misquitta, L., Lee, E., Rotmistrovsky, K., Greenhut, S. F., Schaefer, C. F., Buetow, K., Bonner, T. I., Haussler, D., Kent, J., Kiekhaus, M., Furey, T., Brent, M., Prange, C., Schreiber, K., Shapiro, N., Bhat, N. K., Hopkins, R. F., Hsie, F., Driscoll, T., Soares, M. B., Casavant, T. L., Scheetz, T. E., Brown-stein, M. J., Usdin, T. B., Toshiyuki, S., Carninci, P., Piao, Y., Dudekula, D. B., Ko, M. S., Kawakami, K., Suzuki, Y., Sugano, S., Gruber, C. E., Smith, M. R., Simmons, B., Moore, T., Waterman, R., Johnson, S. L., Ruan, Y., Wei, C. L., Mathavan, S., Gunaratne, P. H., Wu, J., Garcia, A. M., Hulyk, S. W., Fuh, E., Yuan, Y., Sneed, A., Kowis, C., Hodgson, A., Muzny, D. M., McPherson, J., Gibbs, R. A., Fahey, J., Helton, E., Ketteman, M., Madan, A., Rodrigues, S., Sanchez, A., Whiting, M., Madari, A., Young, A. C., Wetherby, K. D., Granite, S. J., Kwong, P. N., Brinkley, C. P., Pearson, R. L., Bouffard, G. G., Blakesly, R. W., Green, E. D., Dickson, M. C., Rodriguez, A. C., Grimwood, J., Schmutz, J., Myers, R. M., Butterfield, Y. S., Griffith, M., Griffith, O. L., Krzywinski, M. I., Liao, N., Morin, R., and Palmquist, D. (2004) The status, quality, and expansion of the NIH full-length cDNA project: the mammalian gene collection (MGC). *Genome Res. 14*, 2121–2127.

37. Witt, A. E., Hines, L. M., Collins, N. L., Hu, Y., Gunawardane, R. N., Moreira, D., Raphael, J., Jepson, D., Koundinya, M., Rolfs, A., Taron, B., Isakoff, S. J., Brugge, J. S., and LaBaer, J. (2006) Functional proteomics approach to investigate the biological activities of cDNAs implicated in breast cancer. *J. Proteome Res. 5*, 599–610.

38. Reinke, A. W., Grant, R. A., and Keating, A. E. (2010) A synthetic coiled-coil interactome provides heterospecific modules for molecular engineering (submitted for publication).

39. Amoutzias, G. D., Veron, A. S., Weiner, J., III, Robinson-Rechavi, M., Bornberg-Bauer, E., Oliver, S. G., and Robertson, D. L. (2007) One billion years of bZIP transcription factor evolution: conservation and change in dimerization and DNA-binding site specificity. *Mol. Biol. Evol. 24*, 827–835.

40. Kataoka, K., Fujiwara, K. T., Noda, M., and Nishizawa, M. (1994) MafB, a new Maf family transcription activator that can associate with Maf and Fos but not with Jun. *Mol. Cell. Biol. 14*, 7581–7591.

41. Acharya, A., Rishi, V., Moll, J., and Vinson, C. (2006) Experimental identification of homodimerizing B-ZIP families in *Homo sapiens*. *J. Struct. Biol. 155*, 130–139.

42. Chen, W.-J., Lewis, K. S., Chandra, G., Cogswell, J. P., Stinnett, S. W., Kadwell, S. H., and Gray, J. G. (1995) Characterization of human E4BP4, a phosphorylated bZIP factor. *Biochim. Biophys. Acta 1264*, 388–396.

43. Adya, N., Zhao, L. J., Huang, W., Boros, I., and Giam, C. Z. (1994) Expansion of CREB's DNA recognition specificity by Tax results from interaction with Ala-Ala-Arg at positions 282−284 near the conserved DNA-binding domain of CREB. *Proc. Natl. Acad. Sci. U.S.A. 91*, 5642–5646.

44. Hogan, M., R., Cockram, G., P., and Lu, R. (2006) Cooperative interaction of Zhangfei and ATF4 in transactivation of the cyclic AMP response element. *FEBS Lett. 580*, 58–62.

45. Ubeda, M., Wang, X. Z., Zinszner, H., Wu, I., Habener, J. F., and Ron, D. (1996) Stress-induced binding of the transcription factor CHOP to a novel DNA control element. *Mol. Cell. Biol. 16*, 1479–1489.

46. Hivin, P., Arpin-Andre, C., Clerc, I., Barbeau, B., and Mesnard, J.-M. (2006) A modified version of a Fos-associated cluster in HBZ affects Jun transcriptional potency. *Nucleic Acids Res. 34*, 2761–2772.

47. Lefort, S., Soucy-Faulkner, A., Grandvaux, N., and Flamand, L. (2007) Binding of Kaposi's sarcoma-associated herpesvirus K-bZIP to interferon-responsive factor 3 elements modulates antiviral gene expression. *J. Virol. 81*, 10950–10960.

48. Chang, Y. N., Dong, D. L., Hayward, G. S., and Hayward, S. D. (1990) The Epstein-Barr virus Zta transactivator: a member of the bZIP family with unique DNA-binding specificity and a dimerization domain that lacks the characteristic heptad leucine zipper motif. *J. Virol. 64*, 3358–3369.

49. Matsumoto, J., Ohshima, T., Isono, O., and Shimotohno, K. (2005) HTLV-1 HBZ suppresses AP-1 activity by impairing both the DNA-binding ability and the stability of c-Jun protein. *Oncogene 24*, 1001–1010.

50. Hicks, M. R., Balesaria, S., Medina-Palazon, C., Pandya, M. J., Woolfson, D. N., and Sinclair, A. J. (2001) Biophysical analysis of natural variants of the multimerization region of Epstein-Barr virus lytic-switch protein BZLF1. *J. Virol. 75*, 5381–5384.

51. Kerppola, T. K., and Curran, T. (1994) A conserved region adjacent to the basic domain is required for recognition of an extended DNA binding site by Maf/Nrl family proteins. *Oncogene 9*, 3149–3158.

52. Chen, Y. H., Yang, J. T., and Chau, K. H. (1974) Determination of the helix and beta form of proteins in aqueous solution by circular dichroism. *Biochemistry 13*, 3350–3359.

53. Rauscher, F. J., III, Sambucetti, L. C., Curran, T., Distel, R. J., and Spiegelman, B. M. (1988) Common DNA binding site for Fos protein complexes and transcription factor AP-1. *Cell 52*, 471–480.

54. Oikarinen, J., Hatamochi, A., and de Crombrugghe, B. (1987) Separate binding sites for nuclear factor 1 and a CCAAT DNA binding factor in the mouse alpha 2(I) collagen promoter. *J. Biol. Chem. 262*, 11064–11070.

55. Vinson, C. R., Hai, T., and Boyd, S. M. (1993) Dimerization specificity of the leucine zipper-containing bZIP motif on DNA binding: prediction and rational design. *Genes Dev. 7*, 1047–1058.

56. Cowell, I. G., Skinner, A., and Hurst, H. C. (1992) Transcriptional repression by a novel member of the bZIP family of transcription factors. *Mol. Cell. Biol. 12*, 3070–3077.

57. Moitra, J., Szilak, L., Krylov, D., and Vinson, C. (1997) Leucine is the most stabilizing aliphatic amino acid in the d position of a dimeric leucine zipper coiled coil. *Biochemistry 36*, 12567–12573.

58. Harbury, P. B., Zhang, T., Kim, P. S., and Alber, T. (1993) A switch between two-, three-, and four-stranded coiled coils in GCN4 leucine zipper mutants. *Science 262*, 1401–1407.

59. Campbell, K. M., Sholders, A. J., and Lumb, K. J. (2002) Contribution of buried lysine residues to the oligomerization specificity and stability of the Fos coiled coil. *Biochemistry 41*, 4866–4871.

60. Kuhlmann, A.-S., Villaudy, J., Gazzolo, L., Castellazzi, M., Mesnard, J.-M., and Duc Dodon, M. (2007) HTLV-1 HBZ cooperates with JunD to enhance transcription of the human telomerase reverse transcriptase gene (hTERT). *Retrovirology 4*, 92.

61. Ryseck, R. P., and Bravo, R. (1991) c-JUN, JUN B, and JUN D differ in their binding affinities to AP-1 and CRE consensus sequences: effect of FOS proteins. *Oncogene 6*, 533–542.

62. Katsuoka, F., Motohashi, H., Ishii, T., Aburatani, H., Engel, J. D., and Yamamoto, M. (2005) Genetic evidence that small maf proteins are essential for the activation of antioxidant response element-dependent genes. *Mol. Cell. Biol. 25*, 8044–8051.

63. Vogt, P. K. (2001) Jun, the oncoprotein. *Oncogene 20*, 2365–2377.

64. Pouponnot, C., Sii-Felice, K., Hmitou, I., Rocques, N., Lecoin, L., Druillennec, S., Felder-Schmittbuhl, M. P., and Eychene, A. (2005) Cell context reveals a dual role for Maf in oncogenesis. *Oncogene 25*, 1299–1310.

65. Kataoka, K., Shioda, S., Yoshitomo-Nakagawa, K., Handa, H., and Nishizawa, M. (2001) Maf and Jun nuclear oncoproteins share downstream target genes for inducing cell transformation. *J. Biol. Chem. 276*, 36849–36856.

66. Parkin, S. E., Baer, M., Copeland, T. D., Schwartz, R. C., and Johnson, P. F. (2002) Regulation of CCAAT/enhancer-binding protein (C/EBP) activator proteins by heterodimerization with C/EBP-gamma (Ig/EBP). *J. Biol. Chem. 277*, 23563–23572.

67. Huguier, S., Baguet, J., Perez, S., van Dam, H., and Castellazzi, M. (1998) Transcription factor ATF2 cooperates with v-Jun to promote growth factor-independent proliferation in vitro and tumor formation in vivo. *Mol. Cell. Biol. 18*, 7020–7029.

68. Lu, R., and Misra, V. (2000) Zhangfei: a second cellular protein interacts with herpes simplex virus accessory factor HCF in a manner similar to Luman and VP16. *Nucleic Acids Res. 28*, 2446–2454.

69. Ikushima, S., Inukai, T., Inaba, T., Nimer, S. D., Cleveland, J. L., and Look, A. T. (1997) Pivotal role for the NFIL3/E4BP4 transcription factor in interleukin 3-mediated survival of pro-B lymphocytes. *Proc. Natl. Acad. Sci. U.S.A. 94*, 2609–2614.

70. Doi, M., Nakajima, Y., Okano, T., and Fukada, Y. (2001) Light-induced phase-delay of the chicken pineal circadian clock is associated with the induction of cE4bp4, a potential transcriptional repressor of cPer2 gene. *Proc. Natl. Acad. Sci. U.S.A. 98*, 8089–8094.

71. Lai, C.-K., and Ting, L.-P. (1999) Transcriptional repression of human hepatitis B virus genes by a bZIP family member, E4BP4. *J. Virol. 73*, 3197–3209.